Hindawi Publishing Corporation
Mathematical Problems in Engineering
Volume 2015, Article ID 817241, 9 pages
http://dx.doi.org/10.1155/2015/817241

Research Article

Zoning Modulus Inversion Method for Concrete Dams Based on Chaos Genetic Optimization Algorithm

Hao Gu,[1,2] Zhongru Wu,[1,2] Xiaofei Huang,[1,2] and Jintao Song[1,2]

[1]*State Key Laboratory of Hydrology-Water Resources and Hydraulic Engineering, Hohai University, Nanjing 210098, China*
[2]*National Engineering Research Center of Water Resources Efficient Utilization and Engineering Safety, Hohai University, Nanjing 210098, China*

Correspondence should be addressed to Zhongru Wu; zrwu@hhu.edu.cn

Received 1 April 2015; Accepted 26 May 2015

Academic Editor: Salvatore Caddemi

For dams and rock foundations of ages, the actual mechanical parameters sometimes differed from the design and the experimental values. Therefore, it is necessary to carry out the inversion analysis on main physical and mechanical parameters of dams and rock foundations. However, only the integrated deformation modulus can be inversed by utilizing the conventional inversion method, and it does not meet the actual situation. Therefore, a new method is developed in this paper to inverse the actual initial zoning deformation modulus and to determine the inversion objective function for the actual zoning deformation modulus, based on the dam displacement measured data and finite element calculation results. Furthermore, based on the chaos genetic optimization algorithm, the inversion method for zoning deformation modulus of dam, dam foundation and, reservoir basin is proposed. Combined with the project case, the feasibility and validity of the proposed method are verified.

1. Introduction

In design and construction of major projects, in the past people mostly focused on the planning, design, and construction of the project, and the safety assessment is usually utilized with the traditional positive analysis method [1], but the various parameters of the mathematical model for positive analysis are generally determined by experts experience or experiment. The values of physical and mechanical parameters of dams are the foundation of design and analysis of the operation behavior of dam body, dam foundation, and reservoir basin. But for dams of ages, the actual mechanical parameters differed from the design and experiment. It is often difficult to reflect the overall mechanical behaviors of dams by utilizing the values of mechanical parameters determined by design or experiment [2–4].

Therefore, it is necessary to carry out the inversion analysis of the main physical and mechanical parameters of dam body, dam foundation, and reservoir basin [5, 6]. By utilizing the dam zoning displacement measured data, application of inverse theory and method for quantitative calculation is the basic idea of inversion analysis which can effectively solve the inversion problem for zoning deformation modulus of dam body, dam foundation, and reservoir basin [7]. An inversion analysis model and method are proposed by considering the influence factors of deformation, load, the dam zoning material characteristics, and topographical and geological conditions of dam body, dam foundation, and reservoir basin. Aiming at the shortage of conventional inversion method, the inversion method for zoning deformation modulus of dam body, dam foundation, and reservoir basin is put forward and with the help of chaos genetic optimization algorithm [8], the inversion process can be realized.

2. The Inversion Analysis Method

2.1. The Conventional Inversion Method. For the dam of ages, the elastic modulus of dam body E_c and deformation moduli of dam foundation and reservoir basin E_r, E_b differed with the original design values. If utilized the original design modulus and other mechanical parameters directly for the analysis of dam deformation behavior may result in a big difference with the actual situation. Therefore, the inversion method is needed through the structure analysis and calculation [9, 10] and, based on the measured data of dam displacement to determine the average elastic modulus of dam body, deformation modulus of dam foundation and reservoir basin. The conventional inversion analysis principle is as follows.

2.1.1. Determination of Dam Displacement Field. Within the linear elastic range and under water pressure H, the balance equation [11] of dam system composed by dam, dam foundation, and reservoir basin is

$$[K]\{\delta\} = \{R_H\}. \tag{1}$$

In this equation, $[K]$, $\{\delta\}$, and $\{R_H\}$ are the overall stiffness matrix, node displacement matrix, and node load matrix, respectively. One has

$$\begin{aligned}[K] = &\sum_{e_j\in\Omega_1}[C]_{e_j}^T[K]_{e_j}[C]_{e_j} + \sum_{e_j\in\Omega_2}[C]_{e_j}^T[K]_{e_j}[C]_{e_j} \\ &+ \sum_{e_j\in\Omega_3}[C]_{e_j}^T[K]_{e_j}[C]_{e_j}.\end{aligned} \tag{2}$$

In the above equation, Ω_1, Ω_2, and Ω_3, respectively, represent the calculation domains of dam, dam foundation, and reservoir rock foundation and $[C]_{e_j}$ and $[K]_{e_j}$ represent stiffness transformation matrix and the stiffness matrix of element e_j.

Analysis shows that Poisson ratios μ_c, μ_r, and μ_b of dam, dam foundation, and reservoir basin could be considered as constant parameters due to their small changes. As for the dam system, the geometric properties basically remained unchanged in the loading process. So $[K]$ in (2) can be expressed as follows [12]:

$$\begin{aligned}[K] = &\sum_{e_j\in\Omega_1}[C]_{e_j}^T\left[\overline{K}\right]_{e_j}[C]_{e_j} + \sum_{e_j\in\Omega_2}[C]_{e_j}^T\left[\overline{K}\right]_{e_j}[C]_{e_j} \\ &+ \sum_{e_j\in\Omega_3}[C]_{e_j}^T\left[\overline{K}\right]_{e_j}[C]_{e_j}.\end{aligned} \tag{3}$$

In (3), $[\overline{K}]_{e_j}$ is mainly concerned with Poisson ratio of corresponding part and geometric characteristics.

Node displacement array according to (1) can be expressed as

$$\{\delta\} = [K]^{-1}\{R_H\}, \tag{4}$$

where $\{R_H\}$ is a fixed value under water pressure H. The nodal displacement $f(H,x,y,z)$ can be shown as the sum of displacement caused by deformation $f_c(H,x,y,z)$, $f_r(H,x,y,z)$, and $f_b(H,x,y,z)$ of dam, dam foundation, and reservoir basin. That is,

$$\begin{aligned}f(H,x,y,z) = &f_c(H,x,y,z) + f_r(H,x,y,z) \\ &+ f_b(H,x,y,z).\end{aligned} \tag{5}$$

In (5), H is the depth of the water; x, y, and z are the node coordinates.

Reference [1] shows that node displacement caused by the dam, dam foundation, and reservoir basin is

$$\begin{aligned}f(H,x,y,z) = &\sum_{k=0}^{3(4)}\sum_{l,m,n=0}^{3}A_{klmn}H^k x^l y^m z^n \\ &+ \sum_{k=0}^{3(4)}\sum_{l,m,n=0}^{3}B_{klmn}H^k x^l y^m z^n \\ &+ \sum_{k=0}^{3(4)}\sum_{l,m,n=0}^{3}C_{klmn}H^k x^l y^m z^n.\end{aligned} \tag{6}$$

In (6), A_{klmn}, B_{klmn}, and C_{klmn} are fitting coefficients of node displacement component factors of dam, dam foundation, and reservoir basin under water pressure H.

Dam displacement field can be determined by (6).

2.1.2. Inversion of E_c, E_r, and E_b. Under the assumption of average deformation moduli E_{c0}, E_{r0}, and E_{b0} of dam, dam foundation, and reservoir basin, dam displacement component field caused by deformation of dam, dam foundation, and reservoir basin can be obtained under different water pressure H as $f_{c0}(H,x,y,z)$, $f_{r0}(H,x,y,z)$, and $f_{b0}(H,x,y,z)$ in (5). A_{klmn}, B_{klmn}, and C_{klmn} in (6) can be obtained by utilizing optimization method. Due to the assumption of average deformation modulus of dam, dam foundation, and reservoir basin in structural calculation, each field component should be adjusted to get the real dam displacement field $f(H,x,y,z)$ and the node displacement equation after adjustment is

$$\begin{aligned}f(H,x,y,z) &= Xf_{c0}(H,x,y,z) + Yf_{r0}(H,x,y,z) \\ &\quad + Zf_{b0}(H,x,y,z) \\ &= X\left(\sum_{k=0}^{3(4)}\sum_{l,m,n=0}^{3}A_{klmn}H^k x^l y^m z^n\right) \\ &\quad + Y\left(\sum_{k=0}^{3(4)}\sum_{l,m,n=0}^{3}B_{klmn}H^k x^l y^m z^n\right) \\ &\quad + Z\left(\sum_{k=0}^{3(4)}\sum_{l,m,n=0}^{3}C_{klmn}H^k x^l y^m z^n\right).\end{aligned} \tag{7}$$

In (7), A_{klmn}, B_{klmn}, and C_{klmn} are fitting coefficients after the optimization of node displacement in structural calculation under different water pressure.

Put (3) into (4) and obtain (7) after expansion; the component adjustment coefficients of X, Y, and Z are

$$\begin{aligned}X &= \frac{E_{c0}}{E_c}; \\ Y &= \frac{E_{r0}E_c}{E_{c0}E_r}; \\ Z &= \frac{E_{b0}E_c}{E_{c0}E_b}.\end{aligned} \tag{8}$$

Utilize various measured displacement data to obtain adjustment coefficients X, Y, and Z in (7) through the optimization analysis. Then average elastic modulus of dam body E_c and average deformation moduli of dam foundation and reservoir basin E_r, E_b can be obtained by utilizing (8).

2.2. Zoning Modulus Inversion Method. Since conventional inversion methods can only inverse the integrated modulus of dam, dam foundation, and reservoir basin, the material composition differed. The dam foundation can be divided into different zones, as the dam body and reservoir basin. Therefore, the zoning deformation measured data is utilized to inverse dam zoning elastic modulus, dam foundation zoning, and reservoir basin zoning deformation modulus. The following analyzes the detailed zoning inversion analysis method.

2.2.1. Method for Determining Initial Zoning Modulus. Dam elastic modulus is referred to deformation modulus for the convenience below. Assume that dam, dam foundation, and reservoir basin are divided into n zones, and the corresponding modulus is E_i $(i = 1, 2, \ldots, n)$. For the zone i, the deformation measured data of corresponding zone can most reflect the impact. Make use of deformation measured data to establish deformation safety monitoring model and the equation is similar to (5). Utilize (5) to separate the water pressure component $f_j(H_m)$ from the value of deformation measuring point j in zone i under the action of water head H_m. On the basis of above, assume that the deformation modulus of zone i is E_i' and the rest of moduli of the other zones utilize the design values. Then calculate water pressure component δ_{jH_m} ($j = 1, 2, \ldots, k$, where k is the number of measuring points; $m = 1, 2, \ldots, M$, where M is the number of water pressure components) of measuring point j in zone i under different water level by structure analysis method such as finite element. The equation of δ_{jH_m} is

$$\delta_{jH_m} = F\left(H_m, E_i'\right). \tag{9}$$

Assume

$$Q = \sum_{j=1}^{k} \sum_{m=1}^{M} \left(f_j\left(H_m\right) - x\delta_{jH_m}\right)^2. \tag{10}$$

Minimize Q, without constraint conditions; then

$$x = \frac{\sum_{j=1}^{k} \sum_{m=1}^{M} f_j\left(H_m\right) \delta_{jH_m}}{\sum_{j=1}^{k} \sum_{m=1}^{M} \delta_{jH_m}{}^2}. \tag{11}$$

Assume that the initial value of the actual modulus is E_{0i} in zone i and the equation of x according to its physical meaning is

$$x = \frac{E_i'}{E_{0i}}. \tag{12}$$

Equation (12) can be used to determine the actual initial modulus in zone i as

$$E_{0i} = \frac{E_i'}{x}. \tag{13}$$

2.2.2. Method for Determining Actual Zoning Deformation Modulus. E_{0i} is the initial deformation modulus, which assumes that other zones utilize design values except zone i. It differed from the actual situation, so multipoint deformation measured data combined with the finite element structure analysis results is needed to inverse the actual deformation modulus [13–16]. The inversion method is as follows.

Firstly, the zoning initial actual deformation modulus E_{0i} $(i = 1, 2, \ldots, n)$ obtained above is utilized to calculate deformation value δ_{H_l} of deformation measuring point under effect of different water head H_l with application of structural analysis method. For example, the calculated deformation value of measuring point p in zone i is δ_{ipH_l} as

$$\delta_{ipH_l} = F\left(H_l, E_{0i} \ \ (i = 1, 2, \ldots, n)\right), \tag{14}$$

where δ_{ipH_l}' is the measured deformation value of measuring point p, which is separated by safety monitoring mathematical model from the measured data. Make

$$\begin{aligned} Q &= \sum_{i=1}^{n} \sum_{p_i=1}^{n_{p_i}} \sum_{l=1}^{N} \left(\delta_{ipH_l}' - x_{p_i}\delta_{ipH_l}\right)^2 \\ &= \sum_{i=1}^{n} \sum_{p_i=1}^{n_{p_i}} \sum_{l=1}^{N} \left(\delta_{ipH_l}' - \frac{E_i'}{E_{0i}}\delta_{ipH_l}\right)^2. \end{aligned} \tag{15}$$

In (15), n is the number of zones. n_{p_i} is the number of measuring points in zone i. N is deformation monitoring frequency. The meaning of x_{p_i} is the same as that in (12).

x_{p_i} is the final deformation modulus adjusting coefficient of zone i when Q in (15) reaches the minimum. Then the actual deformation modulus of zone i can be obtained by (13). Therefore, the following focuses on determining method of x_{p_i}, which is also the process of zoning modulus inversion of dam, dam foundation, and reservoir basin.

3. Zoning Modulus Inversion of Dam, Dam Foundation, and Reservoir Basin

Q in (15) is the undetermined parameter. Under the condition of satisfying constraints, get the minimum Q. Then inversing zoning deformation modulus of dam, dam foundation, and reservoir basin is actually an optimization problem [17, 18]. Zoning deformation modulus E_i $(i = 1, 2, \ldots, n)$ is denoted as S vector. That is,

$$S = \left[E_1, E_2, \ldots, E_n\right]^T. \tag{16}$$

Assume

$$Q = S\left(E_i\right) \longrightarrow \min \quad (i = 1, 2, \ldots, n). \tag{17}$$

To meet the end condition

$$E_{i\min} \le E_i \le E_{i\max} \quad (i = 1, 2, \ldots, n). \tag{18}$$

In (18), $E_{i\min}$, $E_{i\max}$ are the minimum and maximum value of E_i, respectively.

The inversion problem of zoning parameters in (16) cannot be directly solved to meet the constraints of (18), which needs positive analysis methods for repeated trial calculation, and finally get the solution of the optimal zoning parameters. This paper applies chaos genetic optimization algorithm [19, 20] to inverse analysis.

In the process of zoning modulus inversion by chaos genetic optimization algorithm, the equation of random disturbance of zoning modulus is

$$E'_k = (1-\alpha) E^* + \alpha E_k. \quad (19)$$

In (19), E^* is the optimal chaotic vector of zoning deformation modulus obtained by mapping the current optimal solution $(E_1^*, E_2^*, \dots, E_n^*)$ to the interval of $[0, 1]$. E_k is the chaotic vector of zoning deformation modulus after iteration for k times. E'_k is the corresponding chaotic vector of zoning deformation modulus after adding random disturbance $(E_1, E_2, \dots, E_n)$. α takes value between 0 and 1. When $(E_1, E_2, \dots, E_n)$ are gradually close to the optimal solution, α takes the smaller value [21].

Under normal circumstances, α can be determined by the following equation:

$$\alpha = 1 - \left[\frac{k-1}{k}\right]^m. \quad (20)$$

In (20), m is the integer according to the optimization objective function and k is the number of iterations [8].

Chaos genetic parameter disturbance method is clear after the random disturbance analysis of zoning deformation modulus above. The following focuses on inversion process and steps of zoning deformation modulus utilizing chaos genetic algorithm.

(1) Initialize zoning deformation modulus. Under the condition of constraint as (18) generates randomly a set of initial values of zoning modulus, $E_{1,i}^0, E_{2,i}^0, \dots, E_{k,i}^0 \in [E_{i\min}, E_{i\max}]$, $i = 1, 2, \dots, n$. n is the number of parameters to be optimized. k is the number of initial values generated by deformation modulus of each zone.

(2) Produce the initial values in chaotic sequence of zoning deformation modulus. Map $E_{j,i}^0$ to the interval $[0, 1]$ via

$$X_{j,i}^0 = \frac{E_{1,i}^0 - E_{i\min}}{E_{i\max} - E_{i\min}}, \quad i = 1, 2, \dots, n; \; j = 1, 2, \dots, k. \quad (21)$$

(3) Produce zoning deformation modulus chaotic sequence of this generation. The sequence $X_{j,i}^{(0,l)}$ $(l = 0, 1, \dots, m)$ is obtained utilizing the Logistic equation with the initial value $X_{j,i}^0$. Among those, $X_{j,i}^0 = X_{j,i}^{(0,0)}$ and m is the number of chaotic iterations.

(4) Generate family members of zoning deformation modulus. After inverse mapping the following sequence is obtained:

$$E_{j,i}^{(0,l)} = E_{i\min} + (E_{i\max} - E_{i\min}) X_{j,i}^{(0,l)},$$
$$i = 1, 2, \dots, n; \; j = 1, 2, \dots, k; \; l = 1, 2, \dots, m. \quad (22)$$

(5) Choose and calculate $F(E_{j,i}^{(0,l)})$. Identify individuals in each zoning deformation modulus family, so that they have the opportunity to become the father generation.

(6) Coding: encode the selected father generation.

(7) Cross: cross according to crossover probability.

(8) Variation: produce variation according to the mutation probability.

(9) Make chaos genetic optimization operations to the individual of highest fitness.

(10) If the new individual fitness is higher than that of the original individual, then replace the original individual; otherwise the individual remains unchanged. Repeat steps (2)~(10), until Q in (15) reaches the minimum. Then zoning deformation modulus inversion results are obtained. The process is shown in Figure 1.

4. Case Study

A concrete hyperbolic arch dam is located in Southwest China. The crest elevation is 1245.0 m, the minimum foundation surface is 950.5 m, and the maximum dam height is 294.5 m. Vertical measuring points are set in different dam sections to measure dam horizontal displacement. Normal water level is 1240 m. The arch dam is divided into 43 sections. Among them, spillway sections are 22 m~26 m and the rest of dam sections are 20 m. Crest width changes gradually from the center to the arch from 12 m to 16 m. The maximum central angle of arch dam is 92.791°. The bottom width of crown cantilever is 73.124 m, arc-height ratio is 3.035, and thickness-height ratio is 0.248.

In order to analyze the effect of reservoir basin deformation on the hyperbolic arch dam, a wide range finite element model of reservoir basin is established. The displacement boundary condition is extracted from finite element model of the near dam area, which is the basis for analyzing the hyperbolic arch dam working behavior under the influence of reservoir basin deformation. This case focuses on the zoning deformation modulus inversion of the near dam area. According to the characteristics of dam foundation, structure, and material, the dam body will be divided into the left bank A, river bed B, and right bank C. According to the geological condition, the dam foundation is divided into 9 zones. The established near dam area finite element model is composed of altogether 142455 elements and 154960 nodes. Among them, 19559 elements and 24889 nodes are for the dam body. The model is shown in Figure 2.

In the process of inversion analysis, the values of measured data are shown as follows: the left bank of the dam (Zone A) utilizes the radial displacement measured data of

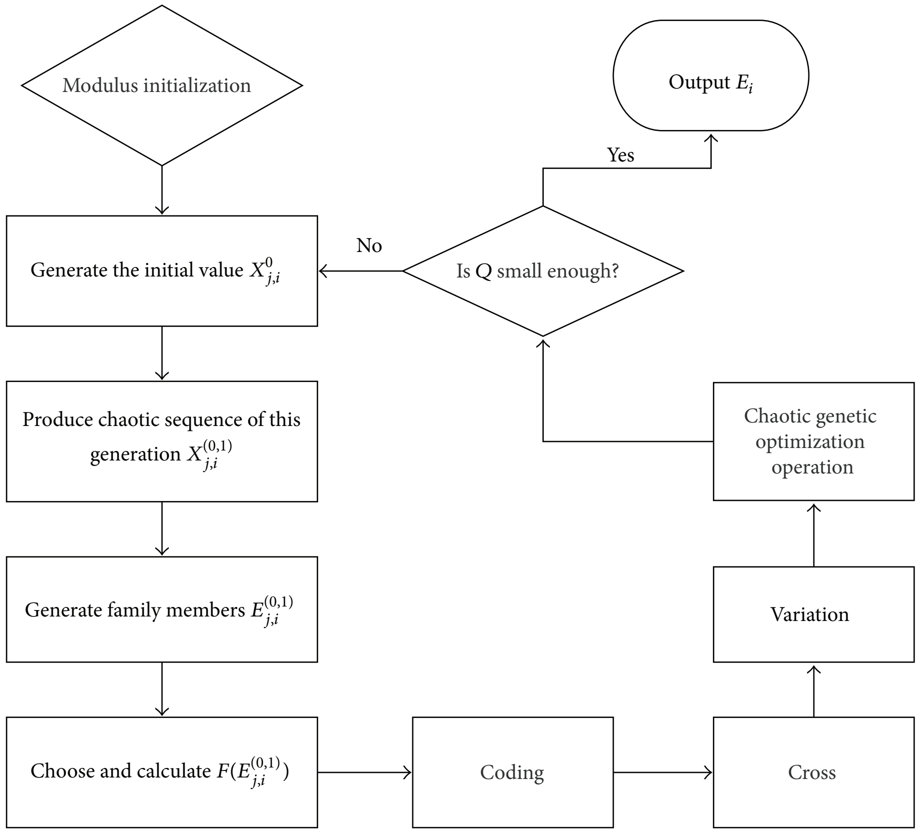

Figure 1: Flow diagram for chaos genetic algorithm to inverse deformation modulus.

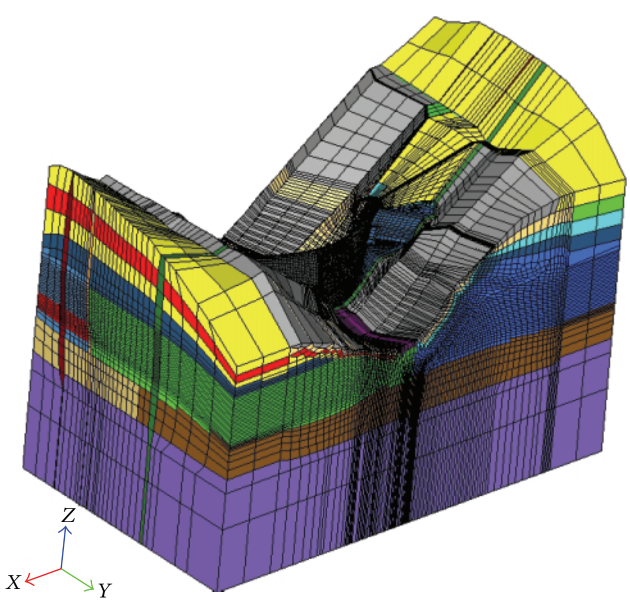

Figure 2: Finite element model of near dam area.

number 1 vertical on dam center and crest. The river bed (Zone B) utilizes the radial displacement measured data of number 2 vertical on dam center and crest, and the right bank of the dam (Zone C) utilizes the radial displacement measured data of number 3 vertical on dam center and crest. The dam foundation is divided into 9 zones. Zone I utilizes the radial displacement measured data from a, b, and c measuring points disposed on Rock I. Zone II utilizes the radial displacement measured data from d, e measuring points disposed on Rock II. Zones $\mathrm{III_a}$, $\mathrm{III_{b1}}$, $\mathrm{III_{b2}}$, and $\mathrm{IV_a}$ utilize the radial displacement measured data from the f, g, h, and i measuring points disposed on the corresponding rocks. Zones F_7, F_{11}, and F_{10} utilize the radial displacement measured data from the j, k, and l measuring points disposed on the corresponding rocks. Selected measured data series is from June 1, 2010, to January 31, 2013. The material types for different zones can be seen in Table 1. Utilizing (9)–(13), based on the radial displacement measured data corresponding to the zoning, the actual initial zoning deformation modulus values obtained by inversion are shown in Table 1. The modulus value range for each zone is also shown in Table 1 according to the modulus obtained by inversion.

Combined with the actual situation of the case, considering the effect of initial value and utilizing radial displacement measured data of the selected representative measured point in each zone from June 1, 2010, to January 31, 2013, the displacement statistical model of each measuring point is established:

$$\delta' = \delta'_H + \delta'_T + \delta'_\theta = a_0 + \sum_{i=1}^{4} \left[a_{1i} \left(H_u^i - H_{u0}^i \right) \right]$$

$$+ \sum_{i=1}^{2} \left[b_{1i} \left(\sin \frac{2\pi i t}{365} - \sin \frac{2\pi i t_0}{365} \right) \right.$$

Table 1: The actual initial modulus and modulus ranges corresponding to different material types.

Material types	Actual initial modulus (GPa)	Modulus range (GPa)
Zone A (dam body)	25.89	10.0–40.0
Zone B (dam body)	25.17	10.0–40.0
Zone C (dam body)	24.25	10.0–40.0
Zone I (rock)	24.56	10.0–40.0
Zone II (rock)	20.17	10.0–30.0
Zone III_a (rock)	14.32	5.0–25.0
Zone III_{b1} (rock)	9.87	5.0–20.0
Zone III_{b2} (rock)	7.05	1.0–15.0
Zone IV_a (rock)	5.21	1.0–15.0
Zone F7 (cataclastic rock)	2.02	1.0–10.0
Zone F11 (slightly weathered)	3.30	1.0–10.0
Zone F10 (slightly weathered)	3.42	1.0–10.0

$$+ b_{2i}\left(\cos\frac{2\pi it}{365} - \cos\frac{2\pi it_0}{365}\right)\Bigg] + d_1(\theta - \theta_0) + d_2(\ln\theta - \ln\theta_0). \tag{23}$$

In (23), δ' is the radial displacement of corresponding measuring point; δ'_H, δ'_T, and δ'_θ are water pressure component, temperature component, and aging component, respectively; a_0 is the constant term; a_{1i} is the water pressure fitting coefficient; b_{1i}, b_{2i} are the temperature factor fitting coefficients; d_1, d_2 are the aging factor fitting coefficients; H_u is the upstream water depth of present measured data; H_{u0} is the upstream water depth of the first measured data in the data series; t is the cumulative days from the initial day to the present day; θ takes $t/100$; θ_0 takes $1/100$.

According to [1], $\sum_{i=1}^{4}[a_{1i}(H_u^i - H_{u0}^i)]$ is utilized to compute the radial displacements caused by the water pressure. Since it is an arch dam, δ'_H has a linear relation with H^4. During the operation period, the temperature of the dam body is affected by air temperature and water temperature, and the temperature of the dam presents a periodic variation. Therefore, the temperature variation of the dam is regarded as a simple harmonic variation, such that $\sum_{i=1}^{2}[b_{1i}(\sin(2\pi it/365) - \sin(2\pi it_0/365)) + b_{2i}(\cos(2\pi it/365) - \cos(2\pi it_0/365))]$ is utilized to compute the radial displacements caused by the temperature. According to the rule of aging variation, at the beginning of the impoundment, the aging changes greatly and then gradually to be steady. In this paper, $d_1(\theta - \theta_0) + d_2(\ln\theta - \ln\theta_0)$ is introduced to compute the radial displacements caused by the aging.

Make use of displacement monitoring mathematical model in (23) to separate water pressure component δ'_H, temperature component δ'_T, and aging component δ'_θ from displacement value of corresponding measuring point. Figure 3 is the radial displacement separation results of number 2 vertical crest measuring point in river bed (Zone B) arch crown beam section. The rest of displacement separation results of measuring points are similar to the above and will not be described here.

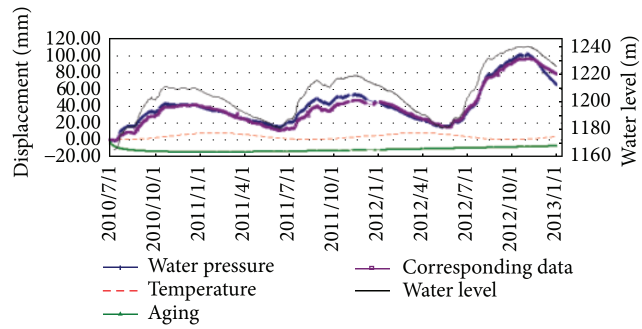

Figure 3: The radial displacement separation results of number 2 vertical crest measuring point.

Table 2: The zoning modulus inversion results.

Material types	Actual deformation modulus inversion (GPa)
Zone A (dam body)	27.91
Zone B (dam body)	27.15
Zone C (dam body)	26.31
Zone I (rock)	25.23
Zone II (rock)	20.73
Zone III_a (rock)	14.59
Zone III_{b1} (rock)	10.09
Zone III_{b2} (rock)	7.58
Zone IV_a (rock)	5.41
Zone F7 (cataclastic rock)	2.07
Zone F11 (slightly weathered)	3.52
Zone F10 (slightly weathered)	3.37

According to the above analysis, the water pressure components can be separated from actual radial displacement of each measuring point by (23), which are δ'_{ipH_l} in (15). Utilizing the initial actual zoning modulus E_{0i} in Figure 1, the finite element analysis model is established to obtain the water pressure components under different water loads, which are δ_{ipH_l} in (15). Then the zoning deformation modulus optimization objective function equation (15) is formed. Finally zoning deformation modulus in this case is obtained utilizing the deformation modulus value range of each zone in Table 1 as the optimization constraints and deformation modulus inversion method based on chaos genetic optimization algorithm. The results are in Table 2. The modulus inversion process of Zone A can be seen in Figures 4–6.

In order to verify the correctness of inversion of the zoning deformation modulus, utilizing zoning deformation modulus in Table 2 as calculation parameters, water pressure component values are calculated by finite element method under different water loads in Table 3, and measured water pressure component values are also shown as the comparison.

Table 3: Calculated values and measured values of radial displacements from vertical measuring points (unit: mm).

Water pressure component	Water pressure component calculated by finite element					Measured water pressure component				
Water level (m)	1165.85	1181	1225	1233	1240	1165.85	1181	1225	1233	1240
Measuring points										
Number 1 vertical dam crest	20.09	30.42	60.58	70.81	79.69	21.61	31.17	61.60	71.34	80.25
Number 1 vertical dam center	15.45	21.96	34.97	38.65	41.21	15.93	22.20	35.52	39.10	41.92
Number 2 vertical dam crest	42.91	56.74	103.05	121.23	141.78	43.10	57.14	104.34	122.10	143.69
Number 2 vertical dam center	37.25	52.17	76.73	84.95	92.61	37.99	52.66	77.11	85.61	93.09
Number 3 vertical dam crest	18.31	25.54	54.68	63.79	72.81	18.74	26.08	55.03	64.11	73.13
Number 3 vertical dam center	14.11	19.05	31.96	35.03	38.14	14.48	19.93	32.41	35.94	38.91

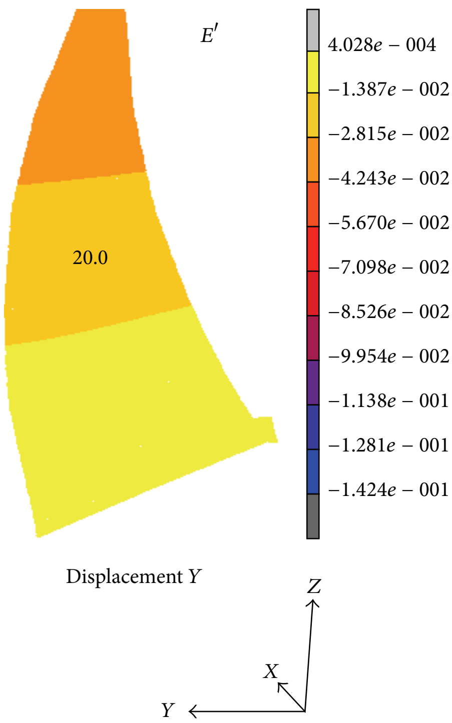

Figure 4: The assumption modulus E'.

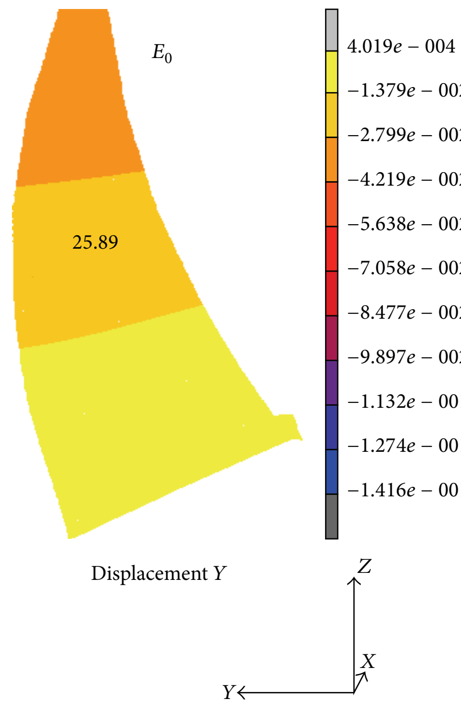

Figure 5: The actual initial modulus E_0.

As can be seen from Table 3, inversed water pressure components of vertical measuring point under different water loads are close to measured water pressure components. The relative errors are all below 5% which reflect the rationality of the zoning deformation modulus inversion results and show the effectiveness of the proposed inversion analysis method in this paper.

5. Conclusions

The inversion method of zoning deformation modulus is mainly focused on, based on the conventional inversion method for the deformation modulus of dam, dam foundation, and reservoir basin. The inversion objective function for zoning deformation modulus is established and the inversion analysis steps are shown. The conclusions are as follows.

(1) Dam displacement field characterization method is developed under the effect of water load based on the basic balance equations. On the basis of this, the method for inversing deformation modulus of dam, dam foundation, and reservoir basin is introduced by utilizing temporal and spatial distribution safety monitoring model of space displacement field. The inversion equations of average deformation modulus of dam, dam foundation, and reservoir basin are derived.

(2) The actual initial zoning deformation modulus of dam, dam foundation, and reservoir basin is put forward, based on the analysis for the defect of conventional inversion method and the comprehensive utilization of the actual displacement measured data and finite element calculation results. Furthermore,

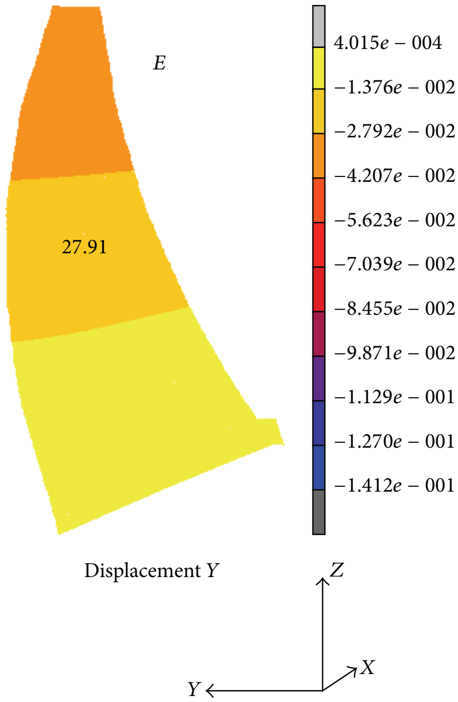

FIGURE 6: The final inversed modulus E.

the inversion objective function for the actual zoning deformation modulus is determined.

(3) The method and implementation steps are proposed to inverse zoning deformation modulus of dam, dam foundation, and reservoir basin based on chaos genetic optimization algorithm. The effectiveness of the zoning inversion method in this paper is verified through the actual project application.

Conflict of Interests

The authors declare that there is no conflict of interests regarding the publication of this paper.

Acknowledgments

This work was supported by the National Natural Science Foundation of China under Grants nos. 41323001, 51139001, 51379068, 51179066, 51279052, and 51209077; Jiangsu Natural Science Foundation under Grants nos. BK20140039, BK2012036; the Research Fund for the Doctoral Program of Higher Education of China under Grants nos. 20120094110005, 20120094130003, and 20130094110010; the Program for New Century Excellent Talents in University under Grant no. NCET-11-0628; the Ministry of Water Resources Public Welfare Industry Research Special Fund Project under Grants nos. 201201038, 201301061; Jiangsu Province "333 High-Level Personnel Training Project" under Grants nos. BRA2011179, BRA2011145; the Project Funded by the Priority Academic Program Development of Jiangsu Higher Education Institutions under Grant no. YS11001; the Fundamental Research Funds for the Central Universities under Grant no. 2014B37414.

References

[1] C. Gu and Z. Wu, *Safety Monitoring of Dams and Dam Foundations-Theories & Methods and Their Application*, Hohai University Press, Nanjing, China, 2006.

[2] A. de Sortis and P. Paoliani, "Statistical analysis and structural identification in concrete dam monitoring," *Engineering Structures*, vol. 29, no. 1, pp. 110–120, 2007.

[3] J. M. W. Brownjohn, "Structural health monitoring of civil infrastructure," *Philosophical Transactions of the Royal Society A*, vol. 365, no. 1851, pp. 589–622, 2007.

[4] C. Gu, D. Qin, Z. Li, and X. Zheng, "Study on semi-parametric statistical model of safety monitoring of cracks in concrete dams," *Mathematical Problems in Engineering*, vol. 2013, Article ID 874629, 9 pages, 2013.

[5] J. Mata, A. Tavares de Castro, and J. Sá da Costa, "Constructing statistical models for arch dam deformation," *Structural Control and Health Monitoring*, vol. 21, no. 3, pp. 423–427, 2014.

[6] Y. Wu, H. Yuan, B. Zhang, Z. Zhang, and Y. Yu, "Displacement-based back-analysis of the model parameters of the Nuozhadu high earth-rockfill dam," *The Scientific World Journal*, vol. 2014, Article ID 292450, 10 pages, 2014.

[7] D. Zheng, L. Cheng, T. Bao, and B. Lv, "Integrated parameter inversion analysis method of a CFRD based on multi-output support vector machines and the clonal selection algorithm," *Computers and Geotechnics*, vol. 47, pp. 68–77, 2013.

[8] S. Gallova, "Neuro-fuzzy learning and genetic algorithm approach with chaos theory principles applying for diagnostic problem solving," in *Proceedings of the World Congress on Engineering*, Lecture Notes in Engineering and Computer Science, 21761, 2009.

[9] N. A. Chernyavskaya, J. Schiff, and L. A. Shuster, "Regularity of the inversion problem for the Sturm-Liouville difference equation. III. A criterion for regularity of the inversion problem," *Journal of Difference Equations and Applications*, vol. 11, no. 3, pp. 245–260, 2005.

[10] L. Goren, M. Fox, and S. D. Willett, "Tectonics from fluvial topography using formal linear inversion: theory and applications to the Inyo Mountains, California," *Journal of Geophysical Research: Earth Surface*, 2014.

[11] S. B. Beheshti-Aval and M. Lezgy-Nazargah, "A finite element model for composite beams with piezoelectric layers using a sinus model," *Journal of Mechanics*, vol. 26, no. 2, pp. 249–258, 2010.

[12] M. Ameri, M. Malakouti, and P. Malekzadeh, "Quasi-static analysis of multilayered domains with viscoelastic layer using incremental-layerwise finite element method," *Mechanics of Time-Dependent Materials*, vol. 18, no. 1, pp. 275–291, 2014.

[13] A. P. Kositsky and J.-P. Avouac, "Inverting geodetic time series with a principal component analysis-based inversion method," *Journal of Geophysical Research B: Solid Earth*, vol. 115, no. 3, Article ID B03401, 2010.

[14] R. L. Thompson, P. Bousquet, F. Chevallier, P. J. Rayner, and P. Ciais, "Impact of the atmospheric sink and vertical mixing on nitrous oxide fluxes estimated using inversion methods," *Journal of Geophysical Research D: Atmospheres*, vol. 116, no. 17, 2011.

[15] H. M. Park, "Viscoelastic flow through an axisymmetric contraction using the grid-by-grid inversion method," *Journal of Applied Mathematics*, vol. 2012, Article ID 420189, 15 pages, 2012.

[16] C. Atkinson and N. D. Aparicio, "Inverse problem method for crack detection in elastic materials under anti-plane strain," *Proceedings of the Royal Society of London, Series A: Mathematical and Physical Sciences*, vol. 445, no. 1925, pp. 637–652, 1994.

[17] M. I. Friswell, "Damage identification using inverse methods," *Philosophical Transactions of the Royal Society A: Mathematical, Physical and Engineering Sciences*, vol. 365, no. 1851, pp. 393–410, 2007.

[18] J. Brinkley, "An investigation of the general term of an important series in the inverse method of finite differences," *Philosophical Transactions of the Royal Society of London*, vol. 97, pp. 114–132, 1807.

[19] X. Wu, X. Huang, G. Fang, and F. Kong, "Optimal operation of multi-objective hydropower reservoir with ecology consideration," *Journal of Water Resource and Protection*, vol. 3, no. 12, pp. 904–911, 2011.

[20] X. Fu, X. Chen, Q. Hou, Z. Wang, and Y. Yin, "An improved chaos genetic algorithm for T-shaped MIMO radar antenna array optimization," *International Journal of Antennas and Propagation*, vol. 2014, Article ID 631820, 6 pages, 2014.

[21] I. Zelinka, "Real-time deterministic chaos control by means of selected evolutionary techniques," *Engineering Applications of Artificial Intelligence*, vol. 22, no. 2, pp. 283–297, 2009.

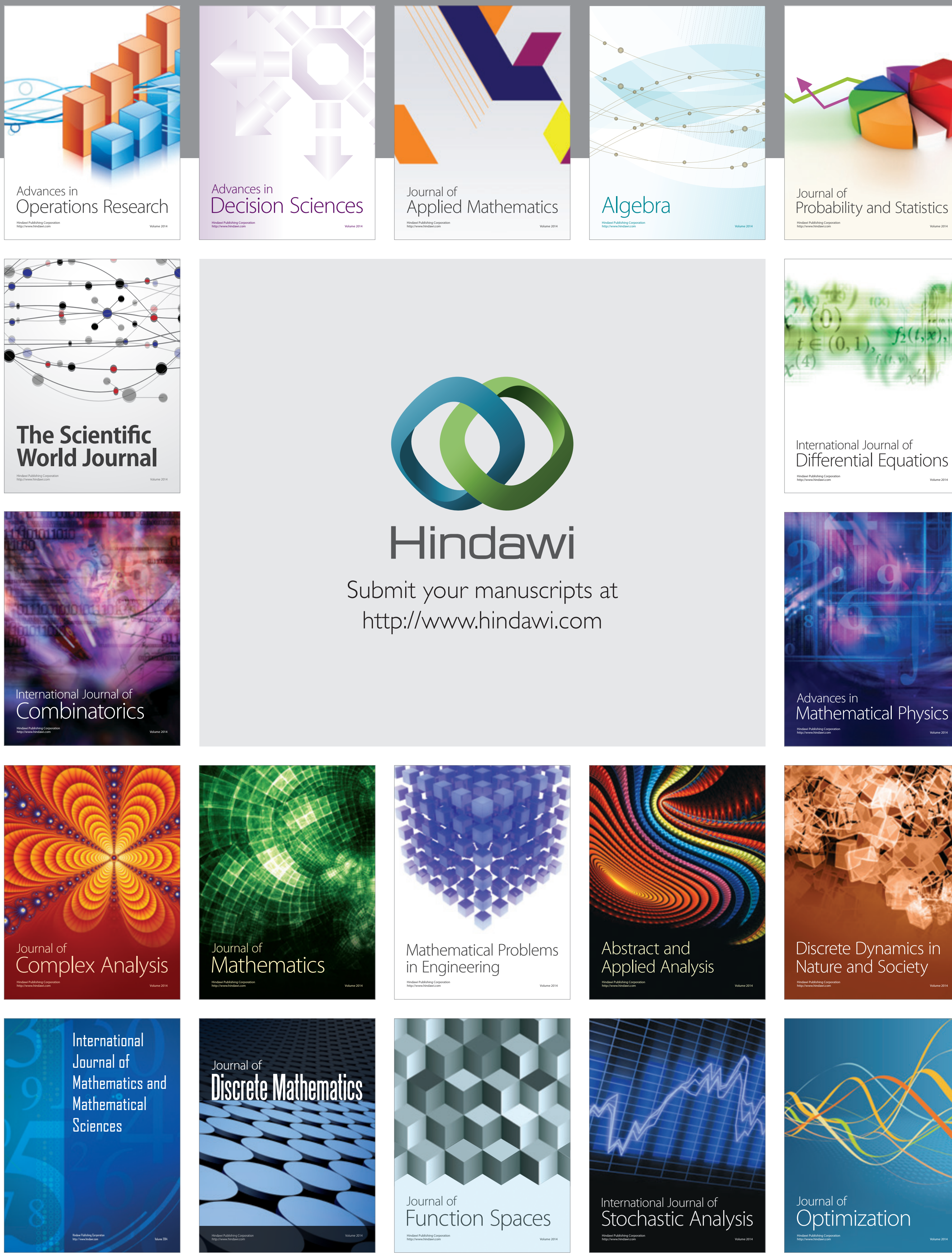
Advances in Operations Research
Advances in Decision Sciences
Journal of Applied Mathematics
Algebra
Journal of Probability and Statistics
The Scientific World Journal
Hindawi
Submit your manuscripts at
http://www.hindawi.com
International Journal of Differential Equations
International Journal of Combinatorics
Advances in Mathematical Physics
Journal of Complex Analysis
Journal of Mathematics
Mathematical Problems in Engineering
Abstract and Applied Analysis
Discrete Dynamics in Nature and Society
International Journal of Mathematics and Mathematical Sciences
Journal of Discrete Mathematics
Journal of Function Spaces
International Journal of Stochastic Analysis
Journal of Optimization